originating at the impact face $t = 2\tau$ are combined additively, is not strictly correct since the equation of state is nonlinear. The uncertainty introduced by this assumption is insignificant.

[34]P. C. Lysne, J. Geophys. Res 75, 4375 (1970).
[35]P. C. Lysne, J. Appl. Phys. 41, 351 (1970).

Radial Distribution Function of an Amorphous Mn-P-C Alloy*

Ashok K. Sinha† and Pol Duwez
W. M. Keck Laboratory of Engineering Materials, California Institute of Technology, Pasadena, California 91109

(Received 14 December 1970; in final form 26 August 1971)

An amorphous manganese base alloy having the composition $Mn_{0.75}P_{0.15}C_{0.10}$ was synthesized by rapid quenching from the liquid state. Its structure was studied using x-ray diffraction. The interference function $a(K)$ of this alloy is characterized by a shoulder on the high-angle side of the second peak, a feature which has been previously observed in several other amorphous alloys but not in amorphous Ni-Pt-P. Both the atomic distribution function $W(r)$ as well as the radial distribution function (RDF) $[=4\pi r^2\rho(r)]$ contain a split double peak beyond the first maximum. The radius of the first near-neighbor shell is 2.63 Å, and its coordination number is approximately 12. The ratio of second to first near-neighbor average interatomic distances is 1.7. A structural model based upon "dense random packing" of Mn atoms with the metalloids P and C filling up some of the interstices may be appropriate for this alloy.

I. INTRODUCTION

The technique of rapid quenching from the liquid state[1] has been used to synthesize amorphous metallic alloys based on Fe,[2,3] Ni,[4–6] Pd,[4,7,8] Pt,[5,6] and Au.[9] These metals form "deep" eutectics with certain metalloids like B, C, Si, P, and Ge, and the corresponding phase diagrams generally contain a large number of rather complex equilibrium crystalline phases. It may be also noted that all of the above-listed metals are located at or near the end of the 3*d*, 4*d*, and 5*d* transition series. It would be of interest to extend studies on amorphous alloys to those in which the major metallic component lies closer to the middle of the transition series. Such studies may help clarify whether or not a nearly full *d* band of the metallic component plays a role in determining the stability and/or the degree of disorder in amorphous alloy phases.

In the present work, an x-ray structure study has been made of a manganese-base amorphous alloy having the composition $Mn_{0.75}P_{0.15}C_{0.10}$. The magnetic properties of this alloy were the subject of recent investigations.[10,11]

II. EXPERIMENTAL

The starting materials were manganese powder of 99.9+ purity, reagent grade red phosphorus powder and 99.9%-pure graphite powder. The properly mixed alloy components were compacted under 50 000-lb./in.^{2} pressure and then reactively sintered at 500 °C for 5 days in a sealed quartz tube containing He atmosphere. The sintered alloy was then melted by heating up to 1100 °C. Rapid quenching of the melt was effected using the piston and anvil technique.[1] The resulting foils, about 40-μ thick, were brittle and flaky; however, their surfaces were smooth and some pieces were as large as 1.5 cm in diameter. The specimen for x-ray measurements consisted of four such foils stacked together with thinned Duco cement on a bakelite substrate. Such a specimen may be assumed to be infinitely thick[12] for the purpose of x-ray absorption correction. Use of Duco cement contributes to an over-all background which was estimated in the manner described below. The x-ray diffraction pattern was recorded in the reflection mode using MoK_α radiation, and a G.E. diffractometer fitted with a diffracted-beam LiF bent-crystal monochromator, a pulse height analyzer, and a scintillation counter. The diffraction pattern was recorded over a range of diffracting angle, 2θ, from 12° to 160° using scanning rates of 0.02° per 100 sec up to $2\theta = 130°$, and 0.04° per 100 sec thereafter. A beam divergence of 1° was employed for values of 2θ between 12 and 64°, and of 3° between 60° and 160°. The angular overlap region of 60° to 64° was utilized to reduce all measurements to 1° divergence. Since it took about 10 days to record the entire diffraction pattern, it was necessary to check the stabilities of the x-ray tube, counter, and associated electronics in accordance with the procedure established in Ref. 4.

The observed intensity data I_{obs} (in arbitrary units) contain contributions from coherent scattering I_c, Compton modified scattering I_{inc}, and background I_b (which arises from fluorescent radiation, Duco cement, and instrumental instabilities). All of these contributions, in turn, are affected by the polarization factor P and the absorption factor A. Thus,

$$I_{obs}(2\theta) = (I_c + I_{inc} + I_b)\,PA\ . \tag{1}$$

Use of a diffracted-beam monochromator removes most of the fluorescent radiation as well as Compton modified scattering at high angles.[13] The remainder of $I_{inc} + I_b$ acts as the effective background $I_B(2\theta)$. The shape of $I_B(2\theta)$ was experimentally determined in a control experiment where the amorphous Mn-P-C foils were replaced by nearly equal thicknesses of recrystallized Fe-P-C (Mn-P-C became too brittle to handle after re-

crystallization) similarly held together.[3] Using this shape, it was only necessary to make small systematic adjustments in order to get exact values of $I_B(2\theta)$ which would be consistent with Eq. (3) (to be discussed later).

As was stated before, the present specimen (~160 μ thick) may be assumed to be one of infinite thickness, and therefore the absorption factor A is effectively independent of angle 2θ.[12] The polarization factor P for a LiF crystal monochromator may be evaluated as

$$P = (1 + \cos^2 2\beta \cos^2 2\theta)(1 + \cos^2 2\beta)^{-1}, \quad (2)$$

where β is the Bragg angle for the (200) reflecting plane of the LiF crystal used.

The coherently scattered intensity I_c (in arbitrary units) was converted into that in electron units, I_c^{eu} by the high-angle normalization method,[14] in which

$$I_c^{eu} = (I_{obs}/P - I_B)\,\alpha \approx \sum_m x_m f_m^2 \quad \text{for } K > 10 \text{ Å}^{-1}. \quad (3)$$

Here, K is the modulus of the scattering vector and is equal to $(4\pi/\lambda)\sin\theta$, where λ is the x-ray wavelength; α is the normalization constant; m stands for Mn, P, or C; x is the atomic fraction; and f is the scattering factor[15] corrected for anomalous dispersion.[16]

III. RESULTS

Figure 1 shows the coherent intensity I_c^{eu} as a function of K. Also shown for comparison is the average scattering power $\sum_m x_m f_m^2$ which represents the diffracted intensity due to independent scattering by atoms of the alloy. I_c^{eu} and $\sum_m x_m f_m^2$ are fitted at high angles in accordance with Eq. (3). The diffraction pattern consists of smooth broad bands characteristic of an amorphous phase. Any crystalline second phase, if present, would give rise to weak but relatively sharp Bragg-like peaks superimposed upon the amorphous bands.

Using the concept of "pair" correlation,[17] and assigning to each atom m an effective member of scattering electrons N_m in accordance with the relations[18]

$$N_m = f_m(K)/f_e(K), \quad (4)$$

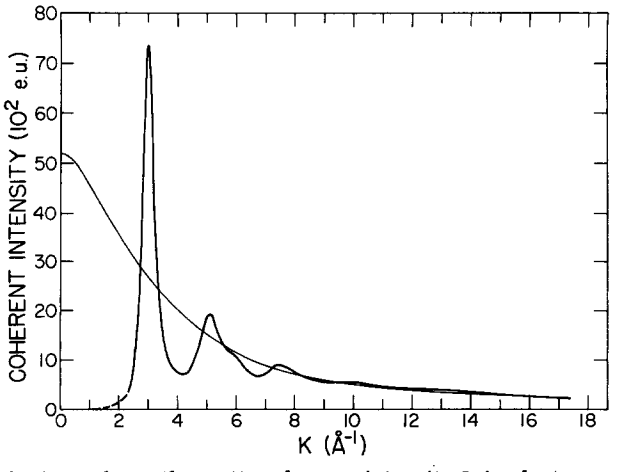

FIG. 1. Coherently scattered x-ray intensity I_c in electron units vs $K(=4\pi/\lambda\,\sin\theta)$ is represented by the oscillating curve. The smoothly varying curve corresponds to $\sum_m x_m f_m^2$, the average scattering power of atoms in $Mn_{0.75}P_{0.15}C_{0.10}$.

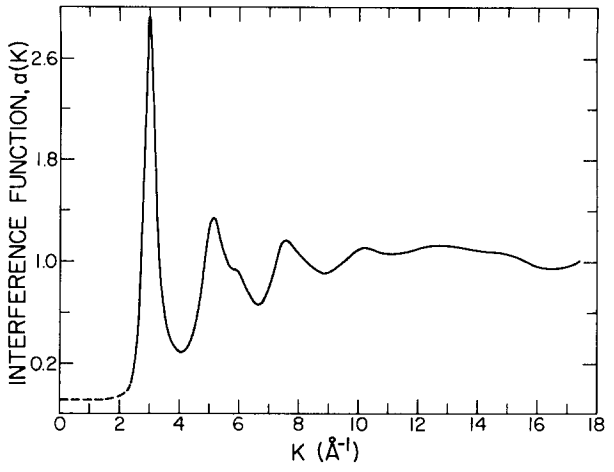

FIG. 2. Interference function $a(K)$ vs K for amorphous $Mn_{0.75}P_{0.15}C_{0.10}$.

$$f_e = (\sum_m x_m f_m)(\sum_m x_m Z_m)^{-1}, \quad (5)$$

where f_e is the effective scattering factor per electron and Z is the atomic number; it is possible to write the following equations for the total x-ray interference function $a(K)$, or the structure factor per atom[6]:

$$K[a(K) - 1] = \int_0^\infty 4\pi r[\rho(r) - \rho_0]\sin Kr\, dr, \quad (6)$$

$$a(K) = (I_c - \sum_m x_m f_m^2)(\sum_m x_m f_m)^{-2}, \quad (7)$$

where $\rho(r)$ is a weighted average[19] atomic density function, and ρ_0 is the average atomic density.

In the case of a ternary alloy, $\rho(r)$ is made up of six pair distribution functions $\rho_{mn}(r)$ in accordance with the following relation[19]:

$$\rho(r) = \sum_m \sum_r \omega_{mn}\rho_{mn}(r), \quad (8)$$

where ω_{mn} is a weighting factor given by

$$\omega_{mn} = x_m N_m N_n (x_m N_m)^{-2}. \quad (9)$$

The total x-ray interference function $a(K)$ is similarly a weighted sum of the six partial interference functions $a_{mn}(K)$.

Figure 2 shows the x-ray interference function $a(K)$ as deduced from Eq. (7) for $Mn_{0.75}P_{0.15}C_{0.10}$. There is a relatively strong peak at $K = 3.00$ Å^{-1} followed by a second one at 5.17 Å^{-1} which has a shoulder at 5.90 Å^{-1}. This is followed by other progressively weaker modulations about the horizontal line $a(K) = 1.0$, which represents a completely uncorrelated structure.

In order to obtain the atomic density function $\rho(r)$ from $a(K)$, it is necessary to perform a Fourier inversion of Eq. (6). This can be done provided ω_{mn} is independent of K. In the case of x-ray diffraction by most alloys, this assumption is not justified, and Fourier inversion of Eq. (6) results in a distribution function $W(r)$ which is the convolution product of the partial pair distribution functions $W_{mn}(r)$ and the Fourier transform of the corresponding weighting factors.[20] Bearing these limitations in mind, Eq. (6) may be Fourier transformed to give

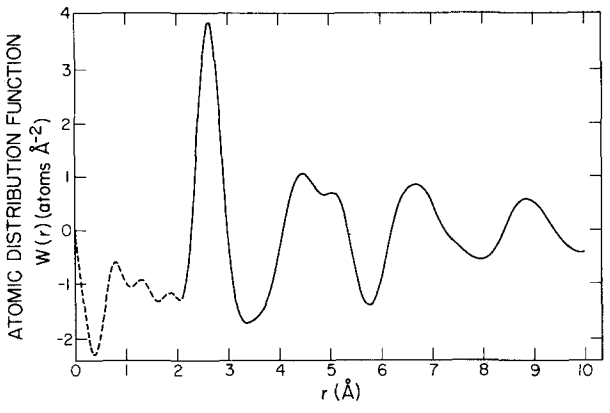

FIG. 3. Atomic distribution function $W(r)$ of amorphous $Mn_{0.75}P_{0.15}C_{0.10}$.

$$4\pi r[\rho(r)-\rho_0]=(2/\pi)\int_0^\infty K[a(K)-1]\sin Kr\,dK. \quad (10)$$

The left-hand side of the above equation is the atomic distribution function $W(r)$, the maxima in which correspond to interatomic distances in the amorphous structure. The distribution function $W(r)$ of amorphous Mn-P-C is shown in Fig. 3. In order to compensate for errors due to termination of the numerical integration in Eq. (10) at a finite value of K, as well as for the experimental inaccuracies in $a(K)$ at higher K values, a convergence factor[18] equal to $\exp(-0.01K^2)$ was applied to the intensity function $K[a(K)-1]$ before carrying out the integration. The spurious ripples present in Fig. 3 at r values less than about 2 Å are due to the relatively small remaining errors in the determination of the normalization constant α. Such errors, however, do not affect the positions of the maxima in $W(r)$. The first peak in Fig. 3 occurs at $r=2.63$ Å. This is followed by a split double peak at 4.47 and 5.07 Å and others at 6.70 and 8.87 Å.

The radial distribution function (RDF) is defined by $4\pi r^2\rho(r)$, where $4\pi r^2\rho(r)dr$ represents the total number of atoms in an interval dr at a radial distance r from the center of any atom m. RDF is simply obtained from Eq. (9) by rearranging the terms:

$$4\pi r^2\rho(r)=4\pi r^2\rho_0+(2r/\pi)\int_0^\infty K[a(K)-1]\sin Kr\,dK\ . \quad (11)$$

The RDF of amorphous $Mn_{0.75}P_{0.15}C_{0.10}$ is shown in Fig. 4 along with the average density curve $4\pi r^2\rho_0$. The first peak in RDF at $r=2.67$ Å is followed by a split double peak at 4.67 Å. The first coordination number (CN) was obtained from the area under the first peak in the RDF:

$$\mathrm{CN}=\int_{r_1}^{r_2}4\pi r^2\rho(r)dr, \quad (12)$$

where r_1 and r_2 are, respectively, the values of r below which RDF = 0, and that corresponding to the first minimum in the RDF. For the present alloy, CN was found to be equal to 12.2.

IV. DISCUSSION

The foregoing results are consistent with the absence of any long-range periodicity in liquid-quenched $Mn_{0.75}P_{0.15}C_{0.10}$. The shoulder on the high-angle side of the second peak in $a(K)$ (Fig. 2) as well as the split double peak beyond the first maximum of $W(r)$ (Fig. 3) and of RDF (Fig. 4), and the presently observed ratio of second to first average interatomic distance r_2/r_1 (~1.7) have been also observed in the case of all previously studied liquid-quenched amorphous alloys[2-4,7,8] except amorphous Ni-Pt-P.[6] A semiquantitative comparison of the degree of structural disorder in various amorphous alloys may be attempted on the basis of the "domain-size" parameters L, which have been estimated, using Scherrer formula, from the width and position of the first band in the corresponding x-ray diffraction pattern.[6] The value of L for $Mn_{0.75}P_{0.15}C_{0.10}$ is 14.5 Å, which is somewhat smaller than that for analogous $Fe_{0.75}P_{0.15}C_{0.10}$, for which $L=15.7$ Å. The smallest L and presumably the highest disorder is observed in the case of $(Ni_{0.20}Pt_{0.80})_{0.75}P_{0.25}$, for which $L=7.6$ Å. In this alloy, the transition metals have almost full d bands. However, judging from the results for Mn-P-C and Fe-P-C, there does not appear to be any consistent trend towards an increase of L (or decrease of disorder) with decreased filling of the d band.

Another structural parameter of interest is the average coordination number whose value (12.2) for amorphous Mn-P-C is close to that present in close-packed structures. In a recently proposed model for the amorphous structure in Ni-P alloys, Polk[21] proposes a Bernal-type dense random packing of the spherical Ni atoms with the P atoms filling up some of the larger holes. This model succeeds in accounting for the splitting of the second peak in the RDF curve and, consequently, for the low value (~1.7) of r_2/r_1 as compared to that (1.8–2.0) present in most liquid metals.[22] It is quite likely that a similar model may be valid for amorphous Mn-P-C with both P and C atoms filling up some of the Bernal polyhedral holes, which are associated with dense random packing of equal-sized spheres. Hasegawa[11] has recently interpreted the magnetic properties of amorphous Mn-P-C in terms of a random mixture of three different kinds of local order corresponding to those present in Mn_3P, Mn_5C_2, and an as yet unknown phase. While this is not incompatible with the presently observed absence of long-range atomic periodicity in amorphous Mn-P-C, any further evaluation of this proposal must await more detailed studies on *local* variations in structure of this alloy.

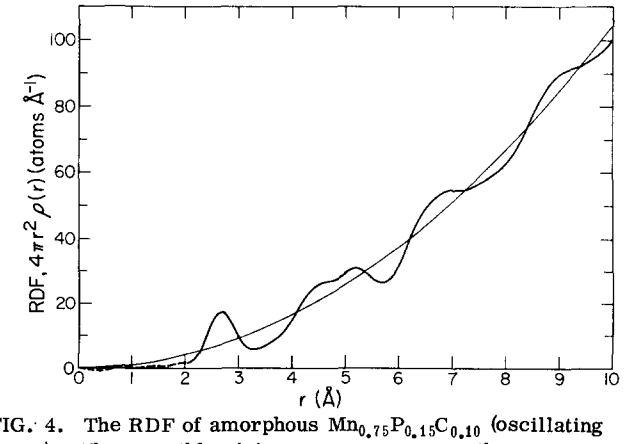

FIG. 4. The RDF of amorphous $Mn_{0.75}P_{0.15}C_{0.10}$ (oscillating curve). The smoothly rising curve represents the average atomic density $4\pi r^2\rho_0$.

*Work supported by the U.S. Atomic Energy Commission.
†Present address: Bell Telephone Laboratories, Murray Hill, N.J. 07974.

[1]Pol Duwez, in *Techniques of Metals Research*, edited by R. F. Bunshah (Interscience, New York, 1968), Vol. I, Part 1, p. 347.
[2]Pol Duwez and S. C. H. Lin, J. Appl. Phys. 38, 4096 (1967).
[3]S. C. H. Lin and Pol Duwez, Phys. Status Solidi 34, 469 (1969).
[4]P. L. Maitrepierre, J. Appl. Phys. 40, 4826 (1969).
[5]A. K. Sinha, Phys. Rev. B 1, 4541 (1970).
[6]A. K. Sinha and Pol Duwez, J. Phys. Chem. Solids 32, 267 (1971).
[7]R. C. Crewdson, Ph.D. thesis (California Institute of Technology, 1968) (unpublished).
[8]Pol Duwez and C. C. Tsuei (unpublished).
[9]H. S. Chen and D. Turnbull J. Appl. Phys. 38, 3646 (1967).
[10]A. K. Sinha, J. Appl. Phys. 42, 338 (1971).
[11]R. Hasegawa, Phys. Rev. B 3, 1631 (1971).
[12]B. D. Cullity, in *Elements of X-Ray Diffraction* (Addison-Wesley, Reading, Mass., 1956).
[13]W. Ruland, Brit. J. Appl. Phys. 15, 1301 (1964).
[14]K. Furukawa, Rept. Prog. Phys. 25, 395 (1962).
[15]D. T. Cromer and J. T. Waber, Acta Cryst. 18, 104 (1965).
[16]D. T. Cromer, Acta Cryst. 18, 17 (1965).
[17]R. W. James, in *The Optical Principles of the Diffraction of X-Rays* (Bell, London, 1962).
[18]B. E. Warren, in *X-Ray Diffraction* (Addison-Wesley, Reading, Mass., 1969).
[19]R. Kaplow, S. L. Strong, and B. L. Averbach, in *Local Atomic Arrangements Studied by X-Ray Diffraction*, edited by J. B. Cohen and J. E. Hilliard (Gordon and Breach, New York, 1966), p. 159.
[20]C. N. J. Wagner, J. Vac. Sci. Technol. 6, 650 (1969).
[21]D. E. Polk, Scripta Met. 4, 117 (1970).
[22]S. Steeb, Fortschr. Chem. Forsch. 10, 473 (1968).

Laser-Induced Stress Waves in Quartz Phenolic*

N. C. Anderholm and R. R. Boade
Sandia Laboratories, Albuquerque, New Mexico 87115
(Received 15 June 1971; in final form 20 August 1971)

Observations of stress-wave generation in quartz phenolic by laser irradiation are reported. A value of the Grüneisen parameter of 0.22 ± 0.05 is found at wavelengths of $\lambda = 0.6943$ and $1.06\ \mu$.

This paper reports observations of stress-wave generation in a two-dimensional quartz phenolic by laser irradiation. The purpose of the study was to measure the effective Grüneisen parameter of the composite. The quartz phenolic used in the experiments was fabricated by the Bendix Corporation, Kansas City Division, from a layered assembly (approximately 270 layer/in.) of fused quartz cloth woven in a square pattern from yarn spun from 8-μ fibers. The assembly was impregnated (under pressure) with phenolic resin, with the concentration of phenolic in the composite being about 30% by weight. Void concentration in the material was less than 1% and the bulk density was 1.77 g/cm^3. Interest in the thermoelastic properties (as well as other properties) of quartz phenolic has been generated because of increasing use of these kinds of materials in the aerospace industry.

The bulk of the experiments considered in this paper were performed using a ruby laser (wavelength = 6943 Å), although a few experiments were performed using a Nd-glass laser (wavelength = 1.06 μ). Incident fluences were varied between 0.07 and 0.41 J/cm^2 and amplitudes of the resulting stress waves ranged up to about 20 bar (1 bar = 10^6 dyn/cm^2).

The Q-switched ruby laser consisted of an oscillator and a $\frac{3}{4} \times 8$-in. amplifier. The Q switching was accomplished using the pulse transmission mode. The output of the laser was a 3-J pulse with a full width at half-maximum of 5 nsec. Fluences were varied by using a negative lens to diverge the beam and by placing an aperture (the sample was directly behind the aperture) at various positions along the beam. Beam uniformity was checked qualitatively by taking burn patterns with commercial "footprint"[1] paper. The aperture was placed in the portion of the radiation field that was most uniform. The fluence was determined by measuring the energy through the aperture (with the sample removed) with a TRG gold-plated cone calorimeter. The time history of the laser pulse was recorded on an oscilloscope by reflecting a portion of the beam by a thin pellicle onto an ITT 114A photodiode. The output of the photodiode was recorded on a 519 Tektronix oscilloscope. The energy through the aperture was measured before and after each shot (or each series of shots) but the photodiode record allowed determination of the constancy of the laser output for each sample irradiation. Sample thicknesses for the ruby-laser experiments were all 1.0 mm. The samples, which were bonded to x-cut quartz crystals[2] (used as stress gauges), were irradiated normal to the plane of the quartz cloth. The diameter of the irradiated area was 2.5 cm, while the diameter of the active area of the quartz gauge was 1.2 cm. With a sample thickness of 1 mm a uniaxial stress in the sample was assured consistent with the heterogenous nature of the sample itself and with a diameter-to-thickness ratio of 4 to 1 for the quartz gauge. No effects due to deviations from uniaxial strain are expected from the transducer. The uniformity of the thickness of the samples was carefully controlled ensuring that deviations were $\leq 2\%$. This assures that effects on the pulse shape due to the tilt of the planes of constant phase with respect to the gauge front plane will be less than 0.006 μsec. Electrical output of the gauges was recorded on a dual-beam oscilloscope. The lens, aperture, and sample/gauge assemblies were